DOI: 10.61782/fa.2023.0917

forum acusticum 2023

AN IMPROVED SCALING METHOD FOR WOODEN FLUE ORGAN PIPES

Péter Rucz[1*] **Elena Esteve Fontestad**[2] **Judit Angster**[2] **András Miklós**[2]

[1] Budapest University of Technology and Economics, Hungary
[2] Fraunhofer Institute for Building Physics, Germany

ABSTRACT

The process of selecting the geometrical dimensions of the pipes in a pipe organ is referred to as scaling. Wooden pipes with rectangular cross-section are usually designed so that their cross-sectional area equals that of the corresponding cylindrical pipe. It often occurs, especially in case of lower registers, that the wooden pipe rank does not fit into the available width, and the pipes are necessarily made narrower. In this case, maintaining the cross-sectional area the same may result in a significant change of timbre due to the increased amount of wall losses.

This paper proposes and examines a scaling method that enables designing narrower wooden pipes with avoiding unwanted changes of the timbre. The approach relies on keeping the wall losses the same as that of the reference cylindrical pipe. The theory of the scaling technique is presented, it is analysed using simplified one-dimensional as well as 3D numerical models. Experimental pipes designed for this study are measured and modelled, proving the applicability of the proposed scaling method.

Keywords: *organ pipes, scaling method, wall losses*

1. INTRODUCTION

When a new pipe organ is planned, the dimensions of each pipe is determined in a process called scaling. The organ builder selects a reference scaling method which prescribes a geometrical progression of diameters along the notes of the musical scale. Then, deviations from the reference are chosen for each stop, based on the desired character of sounds for the registers. Organ builders can also take the room acoustic properties of the church or hall into account during scaling.

For wooden flue pipes with rectangular cross sections, two traditional scaling methods exist. Both methods take the corresponding cylindrical pipe as a reference, see Figure 1. The depth D and width W of the rectangular pipe are chosen such that they either match the diameter $2R$ of the reference pipe ($W = D = 2R$), or that the cross sectional area becomes the same as that of the reference pipe ($DW = R^2\pi$). In case of the latter method, W is chosen such that it equals a given fraction of the circumference of the reference pipe. For diapason pipes, $1/4$ is a common choice, such that $W = 2R\pi/4$.

Figure 1 depicts the structure and parts of a wooden flue organ pipe with an open end. Pressurized air enters the pipe foot through the bore, and forms a jet as it exits the foot through the thin slit called the flue. The air jet interacts with the upper lip, generating pressure waves that travel inside the pipe body and get reflected at the open (or closed) end. The acoustical feedback of the resonator forces a cross-stream movement of the jet leading to a synchronisation and a periodic excitation of the resonator in the steady state of sound generation. The frequency of the pipe is tuned by means of the tuning slot and slide. The geometry of the mouth region is very important in achieving the desired perceived quality of the pipe sound. For wooden pipes, the width of the mouth is equal to the inner width of the pipe, while the height of the mouth (cut-up) is adjusted during the voicing process.

In case of wooden pipes of the lower registers, it occurs relatively often that the series of pipes would not fit into the available space, and it is necessary to make

*__Corresponding author__: rucz@hit.bme.hu.

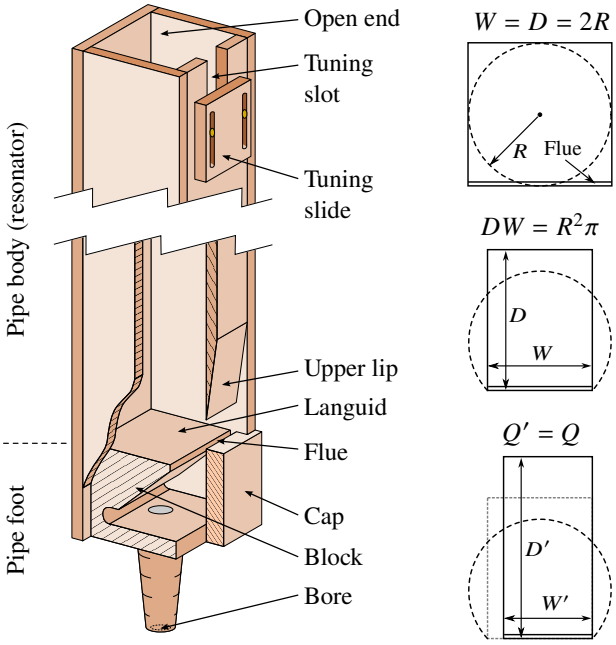

Figure 1. Left: Parts of an open wooden flue pipe. Right: Two traditional and a novel scaling method.

the pipes narrower. This paper examines a scaling approach that allows for designing narrower wooden pipes with maintaining the amount of wall losses constant (see bottom right of Figure 1). The theory of this approach is introduced in Section 2, where a finite element (FE) method with wall losses is also discussed. Section 3 introduces the experimental organ pipes made for this study. The "passive" acoustic behaviour of the pipes is examined by means of laboratory measurements and FE simulations in Section 4. The stationary and transient sound analysis of the experimental pipes are discussed in Section 5. Finally, Section 6 concludes the paper by a short summary.

2. METHODOLOGY

2.1 Theory

Wall losses in wind musical instruments result from friction and thermal diffusion taking place in the boundary layers developing close to the walls. The thickness of the viscous and thermal boundary layers are denoted by δ_v and δ_t, respectively:

$$\delta_v = \sqrt{\frac{2\eta}{\omega\rho_0}} \qquad \delta_t = \sqrt{\frac{2\kappa}{\omega\rho_0 C_p}}, \tag{1}$$

with η, ρ_0, κ, and C_p denoting the dynamic viscosity, equilibrium density, thermal conductivity, and the specific heat at constant pressure, respectively, and ω being the angular frequency.

The combined effect of the boundary layers is expressed by the wall absorption coefficient α, which is found for a cylindrical duct of radius R by an asymptotic approximation [1] as

$$\alpha_\circ \approx \frac{1}{Rc_0}\sqrt{\frac{\eta\omega}{2\rho_0}}\left(1+\frac{\gamma-1}{\sqrt{\mathrm{Pr}}}\right) \approx \frac{3\cdot 10^{-5}\sqrt{f}}{R}, \tag{2}$$

where c_0 is the speed of sound in the free field, γ is the ratio of specific heats, Pr is the Prandtl number, and f is the frequency. Hereafter the subscript $\circ$ refers to the cylindrical geometry. The expression on the right hand side of (2) resulted from the material parameters of dry at the ambient temperature of $T = 20\,^\circ\mathrm{C}$.

At low frequencies, intrinsic and radiation losses are much smaller in organ pipes than wall losses, thus, the latter determine the quality factors of the first few longitudinal eigenmodes of the pipes. The total amount of wall losses in a pipe are proportional to the surface where the losses occur divided by the volume of the pipe. Hence, the quality factor Q becomes inversely proportional to the circumference C and proportional to the cross sectional area S:

$$\frac{1}{2Q} \approx \frac{C\delta L}{SL} = \frac{C\delta}{S} \qquad \text{with} \quad \delta = \frac{1}{2}\delta_v + \frac{\gamma-1}{2}\delta_t. \tag{3}$$

As a consequence, the wall loss coefficient of a rectangular pipe $\alpha_\diamond$ is found from the ratio of the circumferences and $\alpha_\circ$ as:

$$\frac{\alpha_\diamond}{\alpha_\circ} = \frac{2(D+W)}{2\pi R} = \frac{1}{\sqrt{\pi}}\left(\sqrt{\varepsilon}+\frac{1}{\sqrt{\varepsilon}}\right), \tag{4}$$

where $\varepsilon = D/W$ was introduced and the effective radius $R = \sqrt{DW/\pi}$ was utilized assuming that cross sectional areas of the pipes are the same.

From (4) it is immediately seen that $\alpha_\diamond/\alpha_\circ > 1$ and its minimum value is $2/\sqrt{\pi} \approx 1.128$ for $\varepsilon = 1$. By increasing ε, the ratio increases, meaning that narrowing the pipe with keeping the cross sectional area the same increases the amount of wall losses and decreases the quality factor of the most important longitudinal modes.

It follows from (3) that in order to achieve the same quality factor, C/S must be kept constant. Then, for a given reference value of $\varepsilon_1 = D_1/W_1$ and a free parameter $w_n = W_n/W_1$, ε_n is attained as

$$\frac{1}{\varepsilon_n} = \frac{1+\varepsilon_1}{\varepsilon_1} w_n - 1, \tag{5}$$

resulting in the new depth D_n and width W_n that will give the same wall loss coefficient as the reference pipe.

2.2 Finite element model

In the sequel the FE method is applied for modelling wooden flue organ pipes with wall losses. First, the incorporation of wall losses into the acoustical FE technique is discussed, and then the theory presented above is compared to numerical simulations.

Berggren *et al.* [2] proposed an approach that enables treating the boundary layers as boundary conditions (BC) in the FE model. For the simulation domain Ω, the Helmholtz equation is applied, and for the walls Γ_w the BC is written as:

$$\nabla^2 p + k_0^2 p = 0 \qquad \text{in} \quad \Omega \tag{6}$$

$$-\delta_v' \nabla_T^2 p + k_0^2 \delta_t' p + \frac{\partial p}{\partial n} = 0 \qquad \text{on} \quad \Gamma_\mathrm{w} \tag{7}$$

where $\delta_v' = \frac{1}{2}(\mathrm{j}-1)\delta_v$, $\delta_t' = \frac{1}{2}(\mathrm{j}-1)(\gamma-1)\delta_t$, with j being the imaginary unit, and $k_0 = \omega/c_0$. The operator ∇_T denotes the gradient vector containing only the tangential components. To make the problem well-posed a natural BC on $\partial\Gamma_\mathrm{w}$ is also required:

$$\boldsymbol{n}_T \cdot \nabla_T p = 0 \qquad \text{on} \quad \partial\Gamma_\mathrm{w}, \tag{8}$$

with $\boldsymbol{n}_T$ denoting the normal vector that is aligned in the tangential direction of Γ_w.

By substituting (7) into the weak form of (6) and performing an integration by parts on Γ_w, the Galerkin method leads to the following discretized form:

$$\left(\mathbf{K} + \delta_v' \mathbf{K}_\mathrm{w}\right) \mathbf{p} - \omega^2 \left(\mathbf{M} - \delta_t' \mathbf{M}_\mathrm{w}\right) \mathbf{p} = -\mathrm{j}\omega \mathbf{A} \mathbf{v}, \tag{9}$$

where $\mathbf{K}$ and $\mathbf{M}$ and the mass and stiffness matrices, $\mathbf{K}_\mathrm{w}$ and $\mathbf{M}_\mathrm{w}$ are stiffness and mass contributions of the boundary layers on Γ_w from (7). The matrix $\mathbf{A}$ results from a boundary term, and $\mathbf{p}$ and $\mathbf{v}$ are the coefficient vectors of the pressure and normal particle velocity fields.

To compare the wall loss coefficients resulting from the FE model with the theory, a closed cylindrical duct with a radius of $R = 20\,\mathrm{mm}$ was simulated first. In the model, the duct is driven by a rigid piston at the input end and has a perfectly rigid termination on the other end. At each testing frequency the length of the duct was taken as $L = 1.05\lambda$, with $\lambda = c_0/f$ being the wavelength in the free field. To avoid the effect of numerical dispersion, the axisymmetric model was discretized by 1 000 elements along L and 20 elements along R.

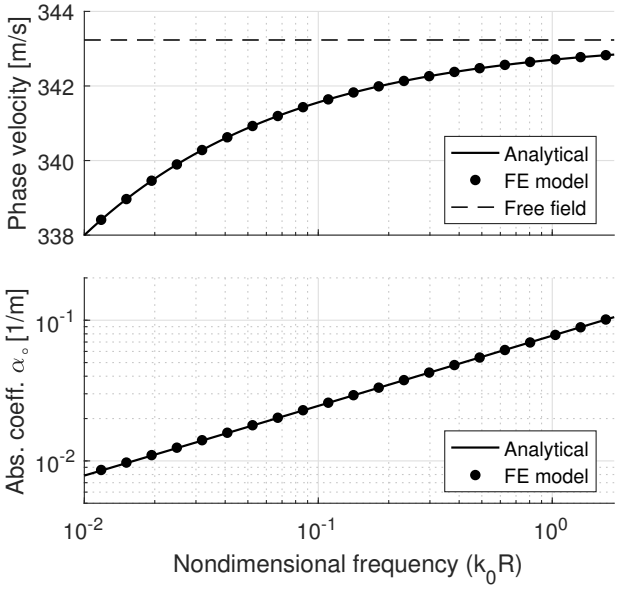

Figure 2. Frequency dependent effects of wall losses in a cylindrical tube with $R = 20\,\mathrm{mm}$.

As the wall losses affect the resulting wave number:

$$k(\omega) = k_0 + \Delta k(\omega) = k'(\omega) - \mathrm{j}\alpha(\omega), \tag{10}$$

the one-dimensional pressure field in the duct is written as

$$p(x) = p^+ \mathrm{e}^{-\mathrm{j}k_0 x} \mathrm{e}^{-\mathrm{j}\Delta k x} + p^- \mathrm{e}^{+\mathrm{j}k_0 x} \mathrm{e}^{+\mathrm{j}\Delta k x}. \tag{11}$$

Finally, Δk is attained by a non-linear least squares fit [3] onto the pressure field in the axis of the tube ($0 \le x \le L$), which results from solving (9) for $\mathbf{p}$. The three complex valued fitted parameters in (11) are p^+, p^-, and Δk.

Figure 2 depicts the comparison of the FE results and the analytical formula of Zwikker & Kosten [4] for the cylindrical pipe, showing an excellent agreement of the models regarding both the phase velocity and the absorption coefficient $\alpha_\circ$. The relative difference between the analytical formula and the FE simulation is $< 0.3\%$ in the frequency range of interest $0.01 \le k_0 R \le 1.84$.

Similar simulations were performed on ducts having rectangular cross sections with different depth to width ratios D/W using 3D FE models. Figure 3 displays the resulting wall loss coefficients compared to a cylindrical duct having the same cross sectional area. Apparently, at very low frequencies ($k_0 R \approx 0.01$) the FE simulation predicts slightly greater wall losses than the theory, with the relative difference being $\approx 1.5\%$. Nevertheless, these

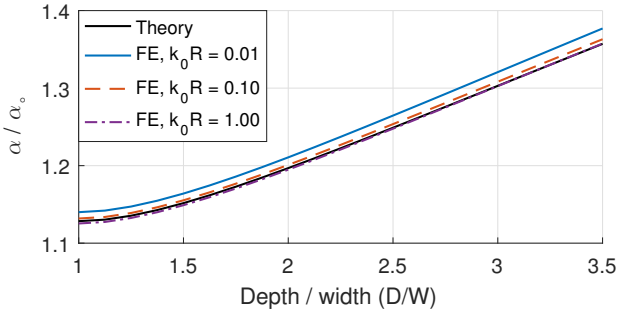

Figure 3. Wall losses of rectangular ducts as a function of $\varepsilon = D/W$. Theory (4) compared to FE.

frequencies are much lower than the fundamental frequencies of the experimental pipes introduced in the next section, which correspond to $k_0 R \approx 0.1$. At higher frequencies a very good match of theory and FE results is found with relative differences of 0.2–0.3%. The agreement of the theory and the numerical model is promising for the FE simulations of complete pipes.

3. EXPERIMENTAL PIPES

Two series of experimental pipes were built by the company Famiglia Artigiana Fratelli Ruffatti, located in Padua, Italy. Both series are open pipes with a nominal tuning to 4′ C, i.e., ≈ 131 Hz. The first series of pipes was scaled, tuned, and voiced by the renowned organ builder Francesco Ruffatti. The first pipe is scaled by taking the width of the mouth as $4/16$ of the circumference of a reference cylindrical diapason pipe, and cut-up H_m is taken as $2/7$ of the width. Then, the width is decreased gradually in the series by taking $4/17$, $4/18$, $4/19$, and $4/20$ of the reference circumference as the width of the pipe, while the depth is increased such that the cross sectional area remains the same. As the pipes become narrower, the height of the mouth was increased by the organ builder to keep the perceived loudness of the pipes roughly the same.

Pipes of the second series were scaled using the scaling rule for equal wall losses (5). As a reference ε_1 was taken as D/W of pipe "$4/16$" of the first series, and the parameter w_n decreased gradually from $w_1 = 1.0$ to $w_5 = 0.8$ in steps of $\Delta w = -0.05$. The 2nd series of pipes was not voiced by the organ builder; however, the front side of the pipes were made detachable allowing for changing the cut-up H_m in voicing experiments. When increasing H_m, small pieces of steel U-profiles could be

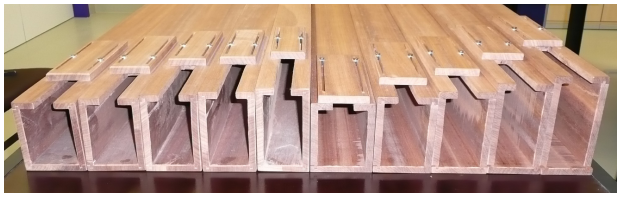

Figure 4. Photo of the top view of the 1st (left) and 2nd (right) series of experimental pipes.

Table 1. Dimensions of experimental pipes in mm.

	Pipe	L	W	D	H_m	L_tun	W_tun
1st series	$4/16$	1180	69.8	86.9	18.6	91.3	28.2
	$4/17$	1180	64.6	93.1	21.7	107.2	25.8
	$4/18$	1181	61.2	98.3	20.6	130.4	27.1
	$4/19$	1180	58.1	103.1	23.4	128.5	26.9
	$4/20$	1179	55.3	108.4	25.1	136.5	24.1
2nd series	1	1183	70.1	87.1	20.0	0.0	30.0
	2	1183	64.9	96.6	20.0	50.0	25.8
	3	1184	60.9	105.9	22.0	68.0	26.2
	4	1185	57.8	117.1	23.0	110.0	26.4
	5	1184	55.8	128.8	24.0	148.0	26.4

inserted to fill the gap formed between the front plate and the cap on the foot. Due to the removable fronts, tuning slots and slides were made on the back side for the 2nd series, while they were located on the front for the 1st series.

Figure 4 shows a photo of the two series of pipes beside each other, while Table 1 lists their dimensions. The parameters L_tun and W_tun are the length and width of the tuning slot. The wall thicknesses varied between 10 and 11 mm, the height of the foot was ≈ 72 mm, and the diameter of the foot hole was ≈ 22 mm for all pipes.

4. ACOUSTICAL ANALYSIS

The resonance properties of the pipes of the first series were examined by means of transfer function measurements. The air column inside the pipe body was excited by a loudspeaker located at a distance of ≈ 0.3 m from the open end of the pipe and driven by a logarithmic chirp signal. A B&K 4165 condenser microphone recorded the signal near the open end, while a small Sennheiser KE 4-211-2 electret probe microphone was inserted into a hole drilled into the back wall of the pipes at 10 mm distance from the languid. The excitation was provided and both

microphone signals processed by a HP 35670A analyser.

FE simulations were also carried out, modelling the arrangement of transfer function measurements. 3D meshes consisting of linear tetrahedron elements were created using the parametric mesh generation software `Gmsh` [5]. The typical edge length in the mesh is 10 mm inside the pipe, and it is refined to 3 and 5 mm in the mouth and at the open end and tuning slot of the pipes. Free field conditions were emulated using Astley–Leis infinite elements [6], which are projected from a surface of a cylinder that encompasses the whole pipe and contains some of the external air. Exploiting plane symmetry along the width of the pipe, the resulting models contained ≈150 k elements and had ≈50 k degrees of freedom. The loudspeaker was modelled as a simple point source, and a virtual microphone location was taken in the same position as the probe microphone inside the pipe.

The quality factors and the natural frequencies were found by fitting a resonance curve onto the narrow neighbourhood of the peaks of the transfer functions $H(f)$:

$$|H(f)|_i \approx \left| \frac{A_i f_i^2/Q_i}{f_i^2 + \mathrm{j} f_i f/Q_i - f^2} \right|, \qquad (12)$$

with $i = 1, 2, \ldots 10$ denoting the ith peak and A_i, Q_i, and f_i being the corresponding magnitude, quality factor, and eigenfrequency, respectively. The cutoff frequency, i.e., the frequency of the first depth-wise transverse mode, $f_{\mathrm{cut}} \approx c_0/(2D)$ is also found from the transfer functions.

Table 2 displays the measured and simulated resonance properties of the fundamental modes and cutoff of the first pipe series. While the eigenfrequencies show an excellent agreement, the FE model gives 18–29% higher Q values than the experiments. A possible explanation of this deviation is the presence of further sources of loss in the measurement, which are not accounted for in the numerical model, such as the roughness of the wall surfaces and the vibration of the walls. The approximation of (3) gives Q_1 values from 69.2 (pipe $^4/_{16}$) to 65.5 ($^4/_{20}$). All three methods gave a decreasing Q_1 value as D/W increases, with the measurement showing the largest decrease in Q_1. The resulting cutoff frequencies agree well with the theoretical values.

The frequencies of the first 10 peaks were also compared, and an excellent agreement was found with relative differences of 1.2% maximum and < 0.5% average. Thus, the FE method with wall losses and infinite elements proves to be a suitable tool for predicting the resonance properties of flue organ pipes. The FE simulation also highlights the importance of wall losses for the first few longitudinal modes of the resonator. A simulation without wall loss effects results in Q_1 values that are more than 3× greater than that with wall losses. At higher frequencies, radiation losses become higher and the discrepancy between the two models diminishes: above 1 kHz, the difference in Q values is only 10–12%.

Table 2. Measured ans simulated resonance properties of the first series of pipes.

Pipe	Measurement			Simulation		
	f_1 [Hz]	Q_1 –	f_{cut} [Hz]	f_1 [Hz]	Q_1 –	f_{cut} [Hz]
$^4/_{16}$	130.9	66.3	1987	130.8	78.7	1990
$^4/_{17}$	131.0	67.4	1848	132.0	78.3	1844
$^4/_{18}$	131.7	65.5	1740	132.2	76.8	1760
$^4/_{19}$	131.9	63.0	1664	132.6	76.9	1678
$^4/_{20}$	131.7	59.4	1582	132.2	76.1	1596

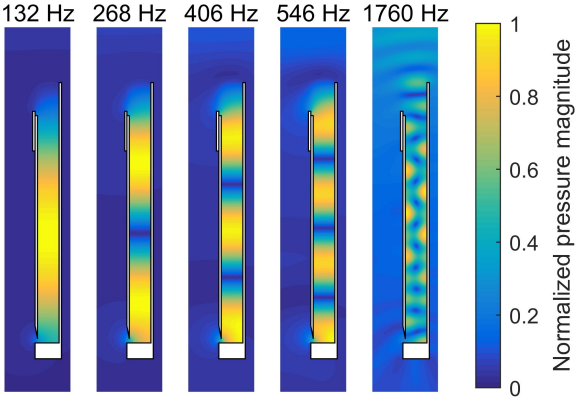

Figure 5. Pressure waveforms of pipe $^4/_{18}$ at the first four eigenfrequencies and at the cutoff.

Figure 5 displays the first few longitudinal mode shapes of pipe $^4/_{18}$ and the effect of the cutoff. As typical to organ pipes with an open end, the pressure maxima of longitudinal modes are shifted slightly towards the mouth from the center of the pipe, as a consequence of the radiation impedances being different at the two openings [7]. The asymmetric radiation pattern due to the presence of the tuning slot is also visible near the open end of the pipe.

The harmonicity of the eigenfrequencies of the resonator is known to have a significant effect on the steady state sound spectrum of flue organ pipes [8,9]. Therefore,

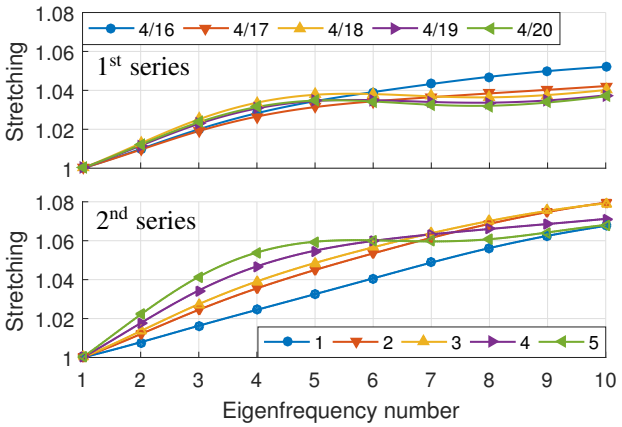

Figure 6. Stretching of the first ten eigenfrequencies of the experimental pipes.

the normalized stretching factors $\mathrm{Str}_n = f_n/(nf_1)$, with f_n denoting the nth eigenfrequency, were extracted from the FE simulations, and shown in Figure 6. For both series of pipes, the stretching factors exhibit an increasing trend with the frequency. Compared to the 1st series, stretching factors of the first few modes gradually increase for the 2nd series, which is a result of increasing the cross sectional area. For higher tuning slot lengths ($L_{\mathrm{tun}} > 100\,\mathrm{mm}$), the stretching factors of higher modes are slightly reduced.

5. SOUND ANALYSIS

The sounds of the experimental pipes were measured and recorded in the anechoic chamber of the Fraunhofer Institute of Building Physics. A model wind system consisting of a blower, regulator, wind ducts, and wind chest was assembled. The pressure in the windchest was set to 700 Pa, which is the voicing wind pressure for the 1st series of pipes. The pipes were sounded by opening a controlled valve in the windchest automatically by a timer. Microphones were located near the open end and the mouth of the pipes, and after amplification their signals were sampled by an 16-bit RME Hammerfall DSP sound card connected to a computer and running at a sampling frequency of 44.1 kHz. In each file, three 10-seconds-long sounds were recorded with 5 s pause between them. First, the steady states were analysed, and the fundamental frequencies f_1 were determined. Then, the recordings were resampled at a rate of $f_s' = 64 f_1$ and the steady state spectra and attack transients were evaluated.

Figure 7 shows the steady state spectra and attack transients of the first pipe series, measured near the mouth of the pipes. The fundamental frequency was 131 Hz in all cases. The pipes only have a few strong partials: beside the fundamental the octave and the third partial (fifth) are relatively strong, other partials are significantly weaker. The attack transients of pipes $^4/_{17}$, $^4/_{18}$, and $^4/_{19}$ are very similar to each other. In each case, the octave has a larger magnitude in the initial stage, and steady state magnitudes of the first three partials are reached after ≈ 0.4–0.5 s, i.e., 50–65 periods. For pipe $^4/_{16}$ a larger overshoot of the octave is observed. The attack of pipe $^4/_{20}$ became very slow, ≈ 0.8 s was needed to reach the steady state magnitude. Here, the fundamental develops first, and the magnitudes of all three partials fluctuate during the attack, which is most probably a consequence of the higher cut-up.

The opinion of the organ builder on the first series of pipes was that the sound colour gradually gets “darker” (more fundamental, less upper harmonics), which he expected due to decreasing the width and increasing the height of the mouth. The organ builder also remarked that with increasing the depth, the acoustical length of the pipe seems to increase (notice that L_{tun} had to be increased gradually to achieve the same pitch, see Table 1).

As the 2nd series of pipes was not voiced by the organ builder, the following approach was pursued. First, different mouth heights were set up using the detachable front sides, and the resulting attack transients were evaluated. Similar attacks were found for mouth heights of 20, 20, 22, 23, and 24 mm for the five pipes, respectively. Then, the pipes were tuned to the same frequency using the tuning slides. Equal frequencies of 126 Hz could be configured with the tuning slot lengths 0, 50, 68, 110 and 148 mm, respectively. After tuning the pipes, new sound recordings were made for evaluation.

Figure 8 depicts the resulting stationary spectra and attack transients. The close similiarity of the levels of the first three partials in the steady state is immediately observed. The gradually increasing stretching factors are also visible in the baselines of the stationary spectra: as the depth of the pipe is increased, the 3rd and 4th eigenfrequencies shift towards higher frequencies from the harmonic partials. A similar, but less pronounced effect is also visible in Figure 7. The attack transients are similar to those of the 1st series: the octave becomes the strongest partial in the initial stage. It has to be remarked that the voicing by the organ builder resulted in quicker attacks and less fluctuation of the levels of the partials.

Table 3 summarizes the levels of the first three partials in the steady state sound of each pipe. The voicing

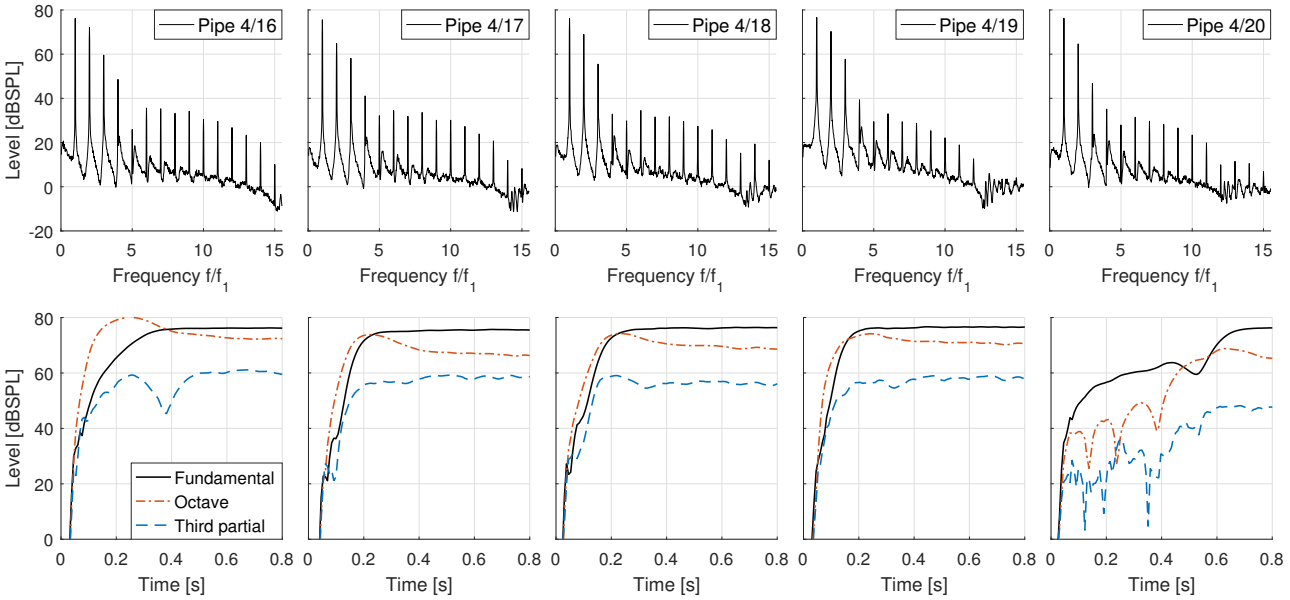

Figure 7. Stationary spectra and attack transients at the mouth for the first pipe series, $f_1 = 131$ Hz.

by the professional organ builder resulted in very similar levels of the fundamental for the first pipe series, while in the second series the differences are somewhat higher. At the same time, the relative level of the octave exhibits larger variations in the first series. In both series, the last pipe (#5) can be considered an outlier, as the 3rd partial became remarkably weaker for these pipes. Concerning the similarity of the first four pipes, the new scaling method can be regarded successful.

6. CONCLUSIONS

This paper examined a possible improvement to the scaling of wooden flue organ pipes with rectangular cross sections. The general idea was to keep the amount of wall losses constant opposed to keeping the cross sectional area constant when reducing the width of the pipe. The theory of wall losses in a rectangular pipe was reviewed and a new scaling rule (5) was established. Two series of experimental pipes using the traditional and new scaling methods were manufactured and analysed by means of laboratory experiments and numerical models. It was found that it is possible to maintain the similarity of the steady state timbre of progressively narrower pipes by applying the proposed scaling method.

The importance of voicing has to be emphasised here. After an experienced organ builder and voicer, Konrad Mühleisen listened to the sounds of the 2nd series of pipes, he immediately objected the slowness of the attacks. He recommended various further voicing adjustments, such as attaching beards to some of the pipes. Nevertheless, he reconsidered his opinion on designing narrower wooden flue pipes with similar timbres from “impossible” to “possible, with further modifications”.

Table 3. Absolute level of the fundamental (L_1) and relative levels of the octave and third partials (ΔL_2, ΔL_3) in the steady state. Values are in dBSPL.

Pipe	1st series			2nd series		
	L_1	ΔL_2	ΔL_3	L_1	ΔL_2	ΔL_3
#1	76.2	−4.0	−16.5	76.1	−12.0	−17.9
#2	75.5	−10.8	−17.4	73.9	−11.5	−15.5
#3	76.1	−7.2	−20.7	75.4	−10.6	−17.8
#4	76.6	−6.3	−18.9	75.2	−13.7	−20.0
#5	76.2	−11.6	−29.5	70.8	−7.2	−31.1

Some remarks are made on the application of the proposed method. As an example, the total width of a 8′ rank of diapason pipes with 3 octaves (37 pipes from 8′ C_2 to 1′ C_5) can be reduced from ≈2.95 to ≈2.51 m, with taking $w = 80\%$. The same method may be applied for de-

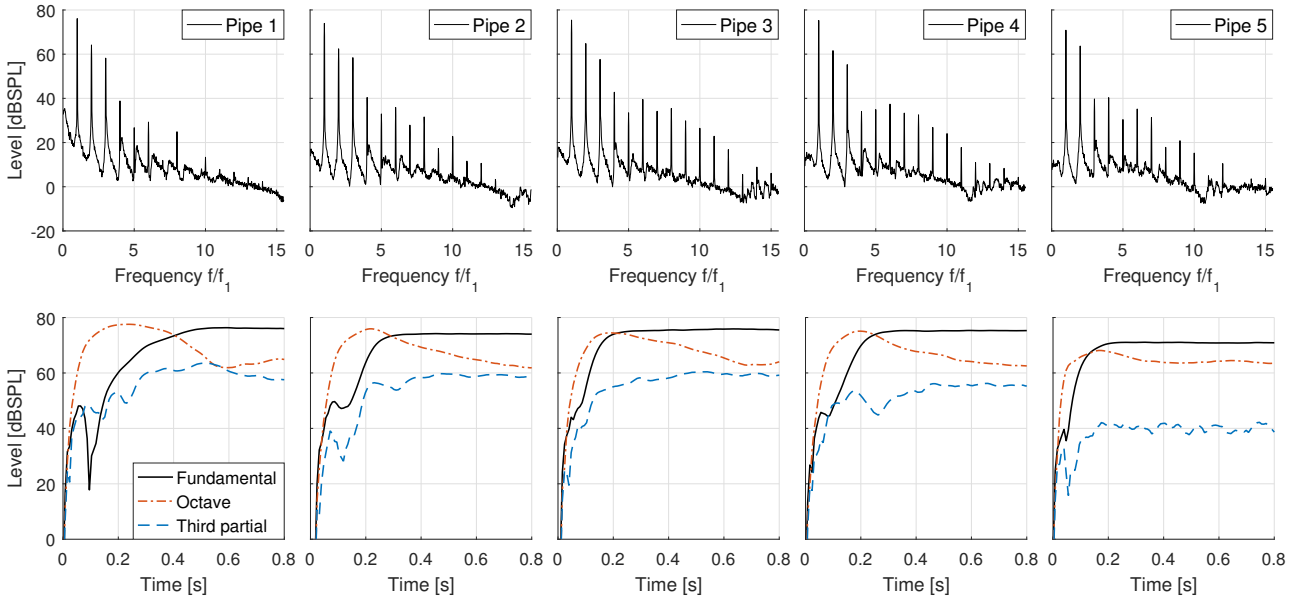

Figure 8. Stationary spectra and attack transients at the mouth for the second pipe series, $f_1 = 126\,\mathrm{Hz}$.

signing stopped wooden flue pipe ranks with rectangular cross sections. Finally, the FE approach can be utilized for investigating the wall losses of different pipe forms.

7. ACKNOWLEDGMENTS

The research was financially supported by the European Commission in the frame of the "INNOSOUND" project (Grant Agreement Ref. No. 222104). Contributions of Francesco Ruffatti (preparation of experimental pipes) and Konrad Mühleisen (participation in voicing experiments) are gratefully acknowledged.

8. REFERENCES

[1] A. H. Benade, "On the propagation of sound waves in a cylindrical conduit," *Journal of the Acoustical Society of America*, vol. 44, no. 2, pp. 616–623, 1968.

[2] M. Berggren, A. Bernland, and D. Noreland, "Acoustic boundary layers as boundary conditions," *Journal of Computational Physics*, vol. 371, pp. 633–650, 2018.

[3] Mathworks Inc., "Documentation of `lsqnonlin`: Solve nonlinear least-squares (nonlinear data-fitting) problems." Last accessed: 4/30/2023.

[4] C. Zwikker and C. W. Kosten, *Sound Abosrbing Materials*. Elsevier, 1949.

[5] C. Geuzaine and J.-F. Remacle, "Gmsh: a three-dimensional finite element mesh generator with built-in pre- and post-processing facilities," *International Journal for Numerical Methods in Engineering*, vol. 79, no. 11, pp. 1309–1331, 2009.

[6] R. J. Astley, G. J. Macaulay, J.-P. Coyette, and L. Cremers, "Three-dimensional wave-envelope elements of variable order for acoustic radiation and scattering: Part I. Formulation in the frequency domain," *Journal of the Acoustical Society of America*, vol. 103, pp. 49–63, 1998.

[7] J. Angster, P. Rucz, and A. Miklós, "Acoustics of organ pipes and future trends in the research," *Acoustics Today*, vol. 13, no. 1, pp. 12–20, 2017.

[8] P. Rucz, T. Trommer, J. Angster, A. Miklós, and F. Augusztinovicz, "Sound design of chimney pipes by optimization of their resonators," *Journal of the Acoustical Society of America*, vol. 133, no. 1, pp. 529–537, 2013.

[9] P. Rucz, F. Augusztinovicz, J. Angster, T. Preukschat, and A. Miklós, "Acoustic behavior of tuning slots of labial organ pipes," *Journal of the Acoustical Society of America*, vol. 135, no. 5, pp. 3056–3065, 2014.